Examination of a Biobased Carbon Nucleating Agent on Poly(lactic acid) Crystallization

Michael R. Snowdon[1,2], Amar K. Mohanty[1,2] and Manjusri Misra[1,2]*

[1]*School of Engineering, Thornbrough Building, University of Guelph, Guelph, N1G 2W1, Ontario, Canada*
[2]*Bioproducts Discovery & Development Centre (BDDC), University of Guelph, Guelph, N1G 2W1, Ontario, Canada*

Received November 01, 2016; Accepted March 27, 2017

ABSTRACT: This article assesses the performance of a biobased carbon as a nucleator using common techniques to stimulate poly(lactic acid) crystallization and enhance the thermal stability of PLA during injection molding. The combination of a biodegradable plasticizer, poly(ethylene glycol) (PEG), along with biobased carbon-rich pyrolyzed biomass char residue and an industrially available microcrystalline talc, were tested for nucleating agent capabilities at additions of 10 wt%. Differential scanning calorimetry (DSC) data demonstrated that the inclusion of the plasticizer could increase the PLA crystalline content with further improvements when nucleating agent was present. With a higher mold temperature, the PLA crystallinity surpassed 40% for the multicomponent formulations. The thermomechanical properties including heat deflection temperature exhibited performance above 100 °C, while the coefficient of thermal expansion was lowered. Optical analysis of the crystal structure showed increased crystallization rate with plasticizer and nucleating agents. The mechanical properties and morphology characteristics are also presented.

KEYWORDS: Biocarbon, mold temperature, tertiary composite, thermal stability, crystallinity

1 INTRODUCTION

Poly(lactic acid) (PLA) is a common biobased and biodegradable thermoplastic biopolymer used in industry. It is conventionally used in packaging applications because of its reasonable barrier properties, good transparency and high strength and modulus. As concerns related to petroleum-based plastics grow, PLA is becoming a more prominent alternative, yet the application range for this material is still limited due to its low thermal stability and impact strength [1]. Other considerations, such as the slow crystallization rate of PLA, also play a role by causing it to have a more amorphous state and therefore low glass transition temperature, reducing the uses it is otherwise capable of [2]. When working at temperatures above the glass transition of PLA, greater than 55–60 °C, the material's crystalline form contributes towards the strength while the amorphous region is of minimal assistance [3]. It is therefore advantageous to have a larger quantity of the crystalline PLA phase to improve the structural rigidity at temperatures above the glass transition. Generally, a crystallinity of around 40% is possible for PLA after an annealing process which is normally done to improve thermal performance of PLA and provide increased modulus [4–6].

When it comes to determining the influential properties that affect the mechanical performance of a thermoplastic there are several morphological characteristics that are considered. These include the ability of a semicrystalline polymer to crystalize, the degree of crystallinity, the type of crystals formed, spherulite size and the molecular weight [7]. Due to the variation in these factors, the processing of molded parts can be widely affected [8]. In the case of injection molding, the formulation and/or the processing conditions may need to be optimized to arrive at the final crystallinity based on the fast cooling rates, from large temperature differences between melt and mold, and the lack of molecular orientation during injection [9].

Typically, there are three different methods which can be utilized to achieve a specific crystallinity for the thermoplastic. The traditional method is to incorporate a nucleating agent that acts to increase the overall number of crystallization sites available within the polymer, thus speeding up the crystallization rate and lowering the spherulite size [10].

**Corresponding author*: mmisra@uoguelph.ca

DOI: 10.7569/JRM.2017.634134

These nucleating agents can boost the generation of nucleation sites for crystallization. This minimizes the molding cycles while also providing the material with a greater modulus [11]. It is considered to be a simple and cost-effective method to enhance the crystallinity of polymers. In the case of PLA, one of the most prominent mineral nucleating agents is talc, which is low cost and has added reinforcement capability. This additive is well known as a physical nucleating agent that can reduce the crystallization half-time, establish a high crystallization rate and provide thermal stability to the molded sample [12]. A secondary method is to include a plasticizer that allows for greater chain mobility, by separating polymer chains through the formation of secondary bonds providing increased free-volume, which leads to improvements in the crystallization rate through reduced viscosity, in turn lowering the activation energy requirements for chain folding during the crystal formation [13]. The addition of a plasticizer not only increases the crystallization rate by enhancing the maneuverability of the polymer chains it also widens the temperature range in which the polymer may crystalize [14]. An example is poly(ethylene glycol), which is one of the top studied plasticizers when working with poly(lactic acid). This is because PEG is able to reduce the glass transition temperature of PLA without altering the melting point, which boosts crystallization [15]. The tertiary option is to vary the processing conditions, whereby the mold temperature may be increased to establish higher crystallinity through manipulation of the crystal nucleation and growth at reduced cooling rates. The final morphology is then dependent on the competing factors such as nucleation, crystal growth, and available amorphous phase. The nucleation is based on the parallel alignment of the polymer chains into small clusters during solidification, which then grow by further ordered chain folding into lamellae [16]. The final spherulites will then be small when a large degree of nucleation sites are present and cooling rates are quick, while slower cooling and reduced nuclei will cause fewer and larger spherulites. This crystallization technique takes advantage of the injection molding parameters. These factors can include the temperature difference between melt and mold, injection rate and holding pressures, which will result in variations of the crystal microstructure [17]. For PLA, there has been some research into the mold temperature and how raising it above 80 °C can enhance the crystallinity, which increases the stiffness and heat deflection temperature of the PLA [6, 18].

This study is focused on examining the combination of effects from the addition of a nucleating agent and a plasticizer on the crystalline component of poly(lactic acid) under differing injection molding temperature conditions. This research hopes to expand the currently limited literature on the joint response of additives on the crystallization kinetics and how they may provide synergistic capabilities. The nucleating ability of the biobased carbon filler was assessed while PEG was used as plasticizer in this study.

2 EXPERIMENTAL

2.1 Materials

Poly(lactic acid) (PLA) injection grade Ingeo 3251D (NatureWorks, USA) with a density of 1.24 g·cm^{-3}, containing 1.4% D-isomer; Poly(ethylene glycol) (PEG) 4000 with a M_w of 3600–4400 and melting range of 58–61 °C (Sigma-Aldrich); A ≤ 400 µm miscanthus-based biochar with a mean particle size of 20–75 µm [19] (Competitive Green Technologies, Canada) produced under slow pyrolysis at 700 °C; Mistron Vapor R talc (Imerys Talc) with a mean particle size of 1.7–2.2 µm.

2.2 Sample Preparation

The polymer pellets of poly(lactic acid) were initially dried in an oven set at 80 °C for a duration of 4 hours before use, having a moisture content of ~ 0.2 wt%. Similarly, the biocarbon was kept in an oven at 105 °C for 24 hours to establish a moisture content of <1.5 wt%. The dry PEG and talc were used as received. Polymer compounding was then done in a DSM Xplore (Netherlands) micro compounder co-rotating twin screw extruder. The polymer and additives were pre-weighed before being melt blended at a temperature of 180 °C for a duration of 2 minutes at a screw speed of 100 rpm. The molten polymer was then transferred at 180 °C to a DSM Xplore micro injection molding machine with a mold temperature of 48 °C or 90 °C. The low mold temperature of 48 °C was used to ensure removal of the stiff composite samples from the mold without breakage or warpage. After the injection cycle of 20 seconds, the molded samples were removed within 30 seconds and left at room temperature (~ 23 °C) to provide short cooling times. The solidified samples were then used for characterization purposes.

2.3 Characterization

This investigation consisted of a control specimen of neat PLA. The loading conditions of the plasticizer and nucleating agents were kept constant at 10 wt%

Table 1 Formulations of PLA containing PEG, biocarbon and talc.

Sample	Mold temp. (°C)	PLA (wt.%)	PEG (wt.%)	Biocarbon (wt.%)	Talc (wt.%)
1	48	100	–	–	–
2		90	–	–	10
3		90	–	10	–
4		90	10	–	–
5		80	10	10	–
6		80	10	–	10
7	90	100	–	–	–
8		90	–	–	10
9		90	–	10	–
10		90	10	–	–
11		80	10	10	–
12		80	10	–	10

throughout the study, as seen in Table 1. This ratio was chosen due to the high cooling rate associated with injection molding, requiring elevated nucleating agent levels and varying processing parameters to provide increased crystallization in the molding process [18].

2.4 Mechanical Analysis

An Instron 3382 Universal testing machine was utilized to measure the strength and moduli of all formulations. The tensile properties were performed following ASTM D638 [20] with type IV specimens at a testing speed of 5 mm/min in ambient conditions. Alternatively, ASTM D790 Procedure A [21] was followed for the flexural properties, which included a span length of 52 mm and 1.4 mm/min crosshead speed. Analysis of the collected data was performed with Bluehill software. The notched Izod impact strengths of the samples were gathered using a TMI Monitor Impact tester based on ASTM D256 [22]. A motorized notching cutter prepared the samples prior to being tested with a 5 ft·lb pendulum. All the values presented are the averages of five or more replicates for each formulation.

2.5 Thermomechanical Analysis

The heat deflection temperatures (HDTs) of the samples were carried out according to ASTM D648 [23] with a 0.455 MPa load in a DMA Q800 (TA Instruments). The samples were measured in three-point bending mode at a heating rate of 2 °C/min between 30 to 150 °C.

The same DMA machine was also utilized to determine the storage modulus of the various samples. The experiments were conducted between –50 °C and 150 °C using a heating rate of 3 °C/min. A dual cantilever clamp was employed with an oscillating amplitude and frequency of 15 µm and 1 Hz, respectively.

A thermomechanical analyzer (TMA) Q400 (TA Instruments), was used to measure the coefficient of linear thermal expansion of the samples. The experiment was conducted following ASTM E831 [24] with the specimen tested perpendicular to the injection molded direction using an expansion probe. The data was obtained at a heating rate of 5 °C/min from room temperature (23 °C) up to 150 °C at a constant applied force of 0.1 N, with the CLTE calculated in the linear region between 80 and 130 °C.

All thermal-mechanical analyses were evaluated using Universal Analysis 2000 software version 4.5A (TA Instruments).

2.6 Thermal Analysis

A differential scanning calorimeter (DSC) Q200 (TA Instruments) was utilized to study the thermal behavior of the samples by measuring the glass transition temperature, T_g, melt temperature, T_m, and crystallinity, χ. The experiment was performed under a nitrogen atmosphere, with 5–10 mg samples. The heating cycle consisted of a ramp rate of 10 °C·min^{-1}, starting at 0 °C and finishing at 240 °C. The temperatures corresponding to the melt, cold crystallization and glass transition (T_g, T_m, T_{cc}) and the related enthalpies (ΔH_m, ΔH_{cc}) were all analyzed from the single heating cycle endothermic curve using Universal Analysis 2000 software version 4.5A (TA Instruments).

The percent crystallinity, χ_c (%), of the samples was carried out using Equation 1:

$$\chi_c(\%) = \frac{\Delta H_m - \Delta H_{cc}}{w_f \times \Delta H_m^0} \times 100\% \quad (1)$$

where ΔH_m^0 is the enthalpy of fusion for 100% crystalline poly(lactic acid), 93.7 J·g^{-1} [25], ΔH_{cc} being the enthalpies of the cold crystallization exotherms, the ΔH_m is the measured enthalpy of fusion of the sample and w_f is the PLA weight fraction within the sample.

2.7 Microscopy Imaging

A Nikon Universal Design Microscope was used for polarized optical microscopy with a controllable hot stage (Linkam LTS 420) for temperature control. The microscope is equipped with a DS-2Mv camera and controlled using NIS-Elements microscope imaging software. The samples were prepared between two microscope glass coverslips and melted at 180 °C. The samples were then cooled at a rate of 25 °C/min to an isothermal temperature of 120 °C, where qualitative analysis of the crystal formation was captured.

For morphological analysis, the fractured surfaces of impact bars were examined with the use of a scanning electron microscope (SEM). Images were taken with a Phenom ProX (Phenom-World BV) with 10 kV set as the accelerating voltage at a magnification of 1000x. The samples were first coated with gold using a Cressington 108 sputter coater to prevent charging.

3 RESULTS AND DISCUSSION

3.1 Thermal Analysis

3.1.1. Differential Scanning Calorimetry (DSC)

To investigate the effects associated with the two nucleating agents, biocarbon and talc, the plasticizer, PEG, and mold temperature on the crystallinity of the injection molded samples, DSC thermograms were analyzed. Figure 1 depicts the melting endotherms for all the samples. As can be seen from the figure, the neat PLA consists of a glass transition temperature, T_g, cold crystallization, T_{cc}, pre-melt crystallization region and a melting zone. When biocarbon or talc was present in PLA using the low mold temperature there was no evident change in the thermal characteristics. The nucleating agent tends to increase the nucleation rate while decreasing the number of crystal nuclei due to space limitations, these offset one another resulting in a crystallinity comparable to neat PLA upon rapid cooling with low mold temperatures.

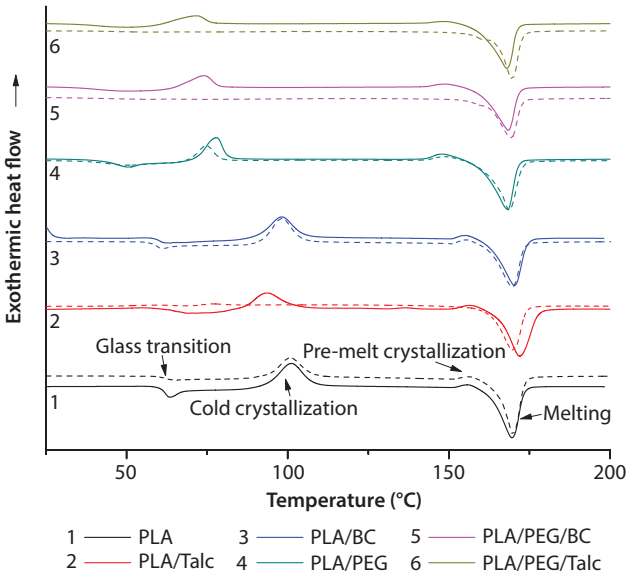

Figure 1 DSC heating cycles of the 48 °C (solid lines) and 90 °C (dashed lines) molded samples.

Table 2 The crystallinity, χ, glass transition, T_g, cold crystallization, T_{cc}, and melt temperatures, T_m, of the PLA samples.

Sample	T_g (°C)	T_{cc} (°C)	T_m (°C)	χ (%)
1	62	101	169	13
2	63	93	173	22
3	60	98	170	15
4	48	78	168	26
5	42	74	168	32
6	42	72	168	37
7	63	101	170	19
8	62	76	170	49
9	60	98	170	12
10	45	75	169	36
11	54	–	169	47
12	47	–	170	41

In the case where the PEG was blended into the PLA matrix, the T_g shifted to a lower temperature, as seen in Table 2. The glass transition temperature of poly(ethylene glycol) is much lower, approximately –22 °C, compared to that of the PLA measured to be 62 °C; therefore, according to the rule of mixtures the new T_g should be 54 °C and the value measured was slightly lower at 48 °C. With the inclusion of the plasticizer PEG, there is an enhancement of the molecular mobility of PLA chains, which reduced the T_g of the PLA blend and also provided greater crystallinity,

as is representative of plasticized thermoplastics [26]. The melting point of PLA was unaffected by the inclusion of the plasticizer, yet the cold crystallization peak at ~100 °C for neat PLA decreased to 75–78 °C due to the presence of the plasticizer. The reduction in cold crystallization can be attributed to the greater maneuverability of the PLA chain segments at lower temperatures which correlated with the drop in the T_g value [27]. The crystallization can therefore begin at a lower temperature when heated. Another justification of the lowered cold crystallization onset is due to pre-existing crystal nuclei that formed during molding [28]. These crystal nuclei, though low in number, provide a denser population of crystals compared to that observed during melt molding, which results in an earlier onset and faster crystallization during the heating process.

For the ternary composites, the plasticizer and nucleating agents provided a favorable combination of nucleation sites and maneuverability to augment the crystallinity above that of the binary systems, while still having a T_g and T_{cc} similar to the plasticized PLA.

When looking at the high mold temperature samples, the PLA still shows the same DSC curve with a minor improvement in its crystallinity. Unexpectedly, the PLA/biocarbon composite did not show any variation in its thermal behavior under these cooling conditions, yet the PLA/talc composite had a major rise in its crystallinity. This is likely a result of the difference in mean particle size of the talc (1.7 µm) relative to the biocarbon (20–75 µm), as it has been shown that smaller dimensional nucleating agents have considerably higher crystallinity capabilities, particularly under high cooling rates [12]. The PLA/talc and PLA/PEG samples had diminished cold crystallization peaks as a greater portion of the PLA was already crystallized upon initial cooling in the mold. The cold crystallization could be completely removed, as seen in the DSC thermograms for the ternary composites. In this scenario, the samples have reached their maximum crystallinity (> 40%) and are more thermally stable above the glass transition temperature.

3.2 Thermomechanical Analysis

3.2.1 Heat Deflection Temperature (HDT)

When it comes to thermal properties of polymeric materials, the softening point known as the heat deflection temperature (HDT) is used to establish the viable thermal application window [29]. Therefore, the larger the HDT value the greater the extent of viable applications and a reduction in sample deformation at elevated temperatures.

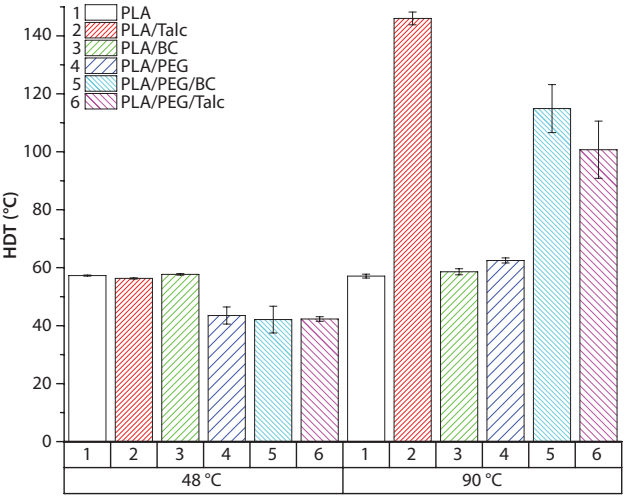

Figure 2 Heat deflection temperature of the PLA samples.

Figure 2 depicts the HDT results for the ten samples tested. The PLA alone had a HDT value of 57 °C. As can be seen, the addition of the talc or biocarbon alone did not impart any change to the HDT. Alternatively, with the inclusion of PEG into the PLA the HDT was lowered because of the reduced glass transition temperature of the blend providing greater flexibility in the sample. The tertiary blends followed the same trend at low mold temperatures with the HDT being decided by the plasticizer in the system.

When looking at the high mold temperature samples, there is a distinct improvement in the HDT for the tertiary composites. The combination of the plasticizer, nucleating agent, and mold temperature provided the proper conditions for elevated crystallinity that resulted in an enhancement of the HDT. The talc and biocarbon composites showed a percent increase of 140 and 174%, respectively, when changing from low to high mold temperature. The most extreme increase in the HDT occurred when only talc was utilized as the nucleating agent. The greater PLA crystallinity of all the high HDT samples gives rise to improved rigidity at temperatures above the glass transition of neat PLA, up to a point where the stiffness of the material can no longer withstand the applied load.

3.2.2 Thermomechanical Analysis (TMA)

The dimensional stability of a polymeric material is important in identifying its range of practical applications under various temperatures and humidity. Depending on the degree of fluctuation in the size of the material there can be alterations in the shape or warpage may occur [30]. One such parameter used to determine the thermal stability of an object is the coefficient of linear thermal expansion (CLTE). Generally

the inclusion of fillers with greater moduli and lower thermal expansion than the matrix under investigation will impart greater thermal stability to the material even above the glass transition temperature, due to the mechanical constraint of the filler [31].

Figure 3 shows the CLTE values for the PLA samples at both low and high mold temperature. The neat PLA had a value of 152 µm/(m·°C), which is comparable to the 171 µm/(m·°C) seen with unfilled PLA above its T_g by Balart *et al*. [32]. The binary systems of either plasticizer or biocarbon filler have increased CLTE values compared to the neat PLA for both mold temperatures. The plasticizer is above its melt temperature, in the range of 80–130 °C, for the specified CLTE measurements and therefore will tend to expand the material throughout the amorphous region of the PLA. In the case of the biocarbon filled composite, the mechanism at play is the increased thermal conductivity associated with the carbon filler, which imparts greater heat conductivity and dissipation throughout the material, reducing the thermal stability of the sample. This is not seen in the talc composite as the volume percentage of talc is lower at 4.7% compared to 9.0% for the biocarbon. Therefore, the transfer of thermal energy from one carbon particle to another is easier than the talc due to the microstructure having a greater interconnectivity from the lower interparticle spacing [33,34]. The talc also provides greater rigidity through its two-dimensional plate-like structure that hinders the expansion of the amorphous polymer, unlike the three-dimensional biocarbon particles.

When both the PEG and biocarbon properties are combined at the low molded temperature the CLTE is highest at 205 µm/(m·°C) versus 152 µm/(m·°C) for pure PLA. It has been shown that fillers with a high thermal conductivity will provide quicker cooling rates and reduce the crystallinity of the composite [35]. Therefore, the observed difference in crystallinity stated previously is related to the increased thermal conductivity along with the cooling rate. However, in the case of the talc-based composite the CLTE remained within standard deviation of the PLA as the talc is a dense filler at 2.8 g·cm^{-3}, compared to the 1.4 g·cm^{-3} for the biocarbon, which is able to provide reinforcement with a low coefficient of thermal expansion, due to its ceramic characteristics.

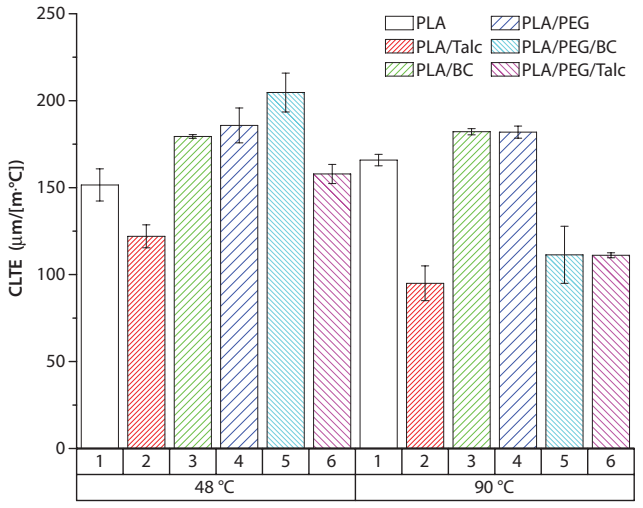

Figure 3 Coefficient of linear thermal expansion of the PLA samples.

The 90 °C molded samples showed the same trend in regards to the single and binary systems for the PLA samples containing PEG and biocarbon. Though, unlike the low molded samples, both the tertiary blends had an improved thermal stability with the CLTE lowering to 111 µm/(m·°C) for both the biocarbon and talc composites. The biocarbon composite had the largest change, with a 46% reduction in CLTE from low to high mold temperature. This reduction is imparted by the high crystallinity of the PLA, which is thermally stable over the heating range, unlike the amorphous portion of the polymer. The amorphous PLA available for expansion was therefore impeded by the crystal regions and stiff fillers. Similarly, the PLA/talc blend also provided a reduced CLTE at the high mold temperature for the same reasons listed above.

3.2.3 *Dynamic Mechanical Analysis (DMA)*

From a commercial standpoint, the storage modulus of injection molded PLA materials can be assessed in terms of how the additives affect the performance. This can occur by the direct increase in modulus or indirectly by changing the crystallinity [36]. The storage moduli of the samples are shown in Figure 4, with the neat PLA having a storage modulus of 3.13 GPa at 25 °C for the low molded sample. The inclusion of the stiff fillers increased this storage modulus to 3.85 GPa, while the soft plasticizer reduced it to 3.09 GPa. The tertiary composite with PEG and biocarbon remained lower at 3.03 GPa while the PLA/PEG/talc composite had a storage modulus of 3.28 GPa at 25 °C. The room temperature storage modulus of the samples prepared at the high mold temperatures had lower moduli compared to the PLA alone, 3.25 GPa, other than the PLA/talc composite, 4.53 GPa. The increased storage modulus is common as talc along with other inorganic fillers have moduli on the order of one magnitude or more compared to the majority of polymers [37]. All samples molded at 48 °C have a major loss of storage modulus above the T_g of the samples, since the minor increase in crystallinity is insufficient in maintaining the elastic response. This occurs earlier for the compounds containing PEG, as the polymeric chains

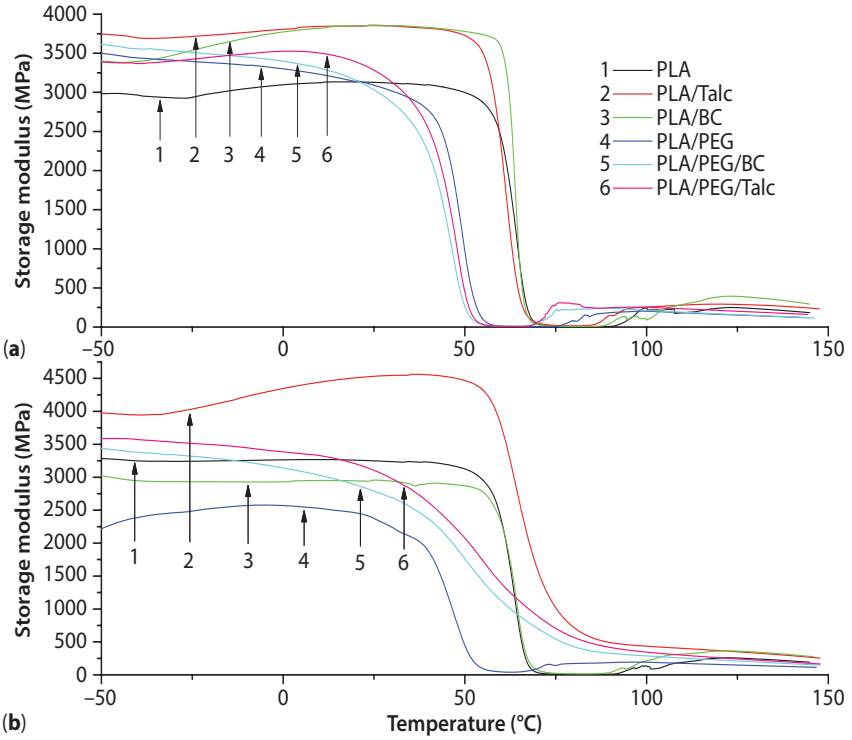

Figure 4 The storage modulus of the PLA-based (**a**) 48 °C and (**b**) 90 °C molded samples.

undergo the glass to rubber transition at a lower temperature, resulting in a decline of matrix stiffness [37]. An increase in the storage modulus in the temperature range of 60–100 °C occurs as a result of the cold crystallization that PLA undergoes in this region [14]. The onset temperature for this increase is lowered when PEG was involved, as seen in the DSC curves.

When regarding the high mold temperature samples, the neat PLA, PLA/PEG and PLA/biocarbon all show the same trend as the low molded samples. These polymeric systems had a loss of storage modulus above their T_g and upon cold crystallization the storage modulus was elevated a small fraction. The PLA/talc and the ternary composites had a gradual decline in their storage modulus above the T_g, with no increase at higher temperatures. This difference is attributed to the high crystallinity and more perfect spherulites present, providing greater rigidity in the sample and removing cold crystallization, which augments the storage modulus [14, 38]. These samples all showed higher storage moduli in the 70–100 °C range versus the lower crystallinity samples, yet the loss in moduli was not fully avoided with the crystallinity differences. The PLA/talc composite showed the least moduli reduction beyond the T_g, correlating well with the largest crystallinity. Only the compounds having crystallinity around the 40% or higher range limited the degree of modulus loss above T_g. Therefore, the enhancement in HDT and stiffness of PLA can be focused on maximizing the crystallinity.

3.3 Mechanical Properties

The mechanical properties, including the tensile, flexural strengths and moduli, were characterized for all the PLA samples and can be seen in Figure 5 and Figure 6. The neat PLA had the highest tensile and flexural strength versus the other samples. This strength is lowered with the inclusion of the nucleating agents due to the low affinity of the matrix to the particulate material which provides little stress transfer under tension. This reduction in strength was more prevalent in the biocarbon than the talc-based composites when using a low mold temperature due to the abundance of sharp edges, non-uniform particle shapes and larger particle sizes that weaken the material from high stress concentration [39]. The plasticizer dropped the strength even further, as it has a lower molecular weight and allows for polymer chains to easily slide past one another [40]. When both the PEG and the nucleating agent were incorporated into the PLA the combination of strength reduction mechanisms decreased the strength by 33–43% from the PLA. The same trend in tensile and flexural strength was evident for the high mold temperature samples with the exception of the PLA/talc composite having

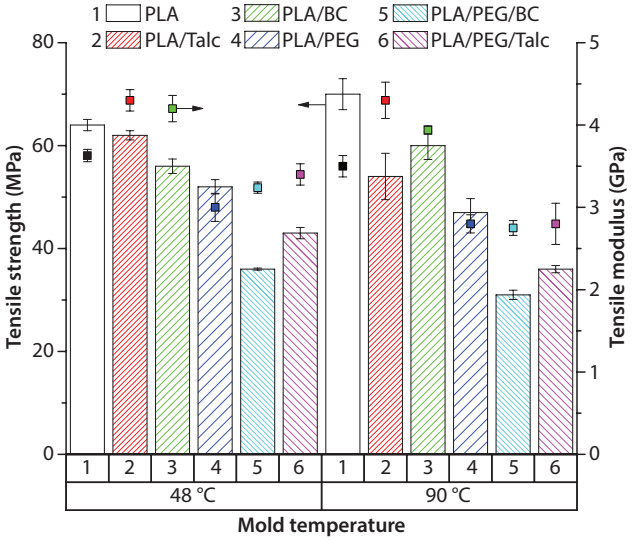

Figure 5 Tensile strengths and moduli of the PLA-based samples at the two mold temperatures.

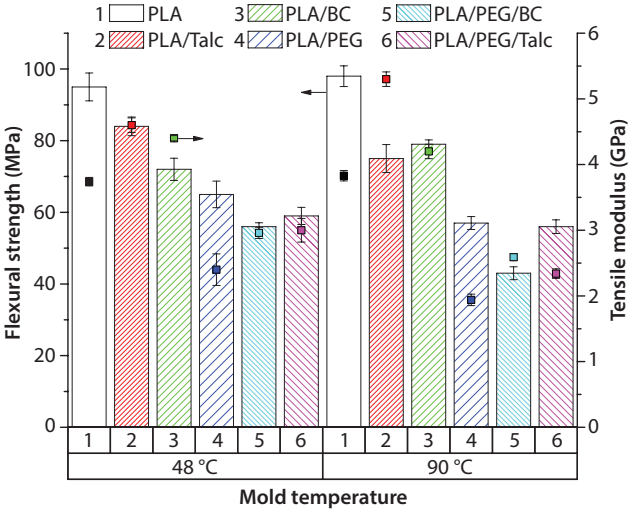

Figure 6 Flexural strengths and moduli of the PLA-based samples at the two mold temperatures.

comparative strength to the PLA/biocarbon as a result of the high crystallinity in this sample [41].

In terms of the modulus, the addition of the stiff nucleating agents provided greater moduli, above 4 GPa, than the pure PLA, ~ 3.6 GPa. In contrast, the PEG, being a softer and more flexible material, reduced the modulus of the blend and composites below that of the PLA. This was seen in both the tensile and flexural moduli for both low and high mold temperatures.

Figure 7 shows the notched Izod impact strength of neat PLA and the PLA blends and composites. All the test specimens underwent complete breaks

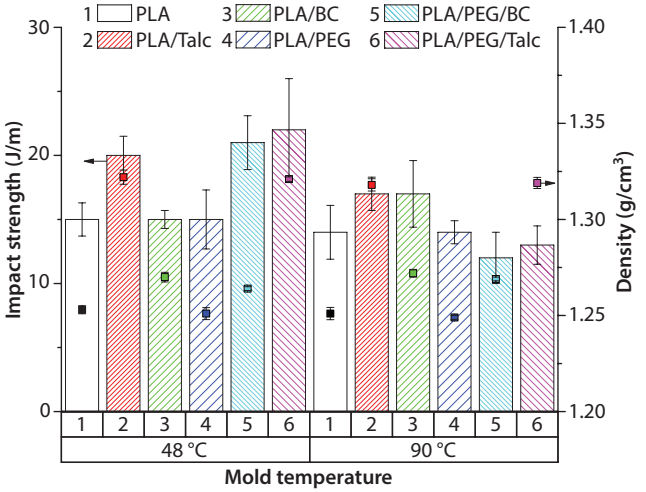

Figure 7 Impact strengths and the densities of the PLA-based samples at the two mold temperatures.

during the investigation. A minor increase in the impact strength was observed only for the PLA/talc composite and ternary composites for the low temperature molded samples. The slight improvement in the impact strength for these samples is associated with the smaller spherulites of PLA formed [42]. When these samples were prepared at the high mold temperature, however, the impact strength of all the samples retained comparable strength to the neat PLA within standard deviation. The impact strength of the material is highly dependent on the crystal morphology and the energy dissipation mechanisms. Therefore, in the high mold temperature samples the impact strength was affected by the crystallinity and the nucleating agent. The brittleness of the samples can be a consequence of imperfect crystals containing microcracks and poor interconnected crystal structure, along with the impeded flexibility of the PLA molecular chains at high crystallinity that reduce the availability of active chains capable of absorbing energy [43, 44]. In addition, the particles forming agglomerates and containing sharp corners produce stress concentration points that impart discontinuity in the matrix and increase the resistance of local plastic deformation, allowing crack propagation to occur quickly [44, 45]

The densities of the various samples are also depicted in Figure 7. The benefit of using biocarbon versus talc is evident here as the percent increase in density from neat PLA is only 1.6% for the biocarbon-based composites, whereas the talc composites have a 5.6% increase. The difference stems from the density of the two nucleating agents. The biocarbon has a density of 1.4 g·cm^{-3}, while the talc has a density of 2.8 g·cm^{-3}, based on rule of mixtures. When it comes to most applications the

lighter the material the better, and talc remains a dense nucleating agent to be used in such circumstances.

3.4 Microscopy Imaging

The polarized optical microscopy images for PLA and its blends and composites crystallized isothermally at 120 °C and the resulting spherulitic morphology is shown in Figure 8 in order to establish an idea of what is occurring for the high mold temperature samples. As it is already known, under quick cooling conditions, such as low mold temperatures, the degree of crystallinity is less with smaller crystallites and vice versa for slow cooling or high mold temperatures [46]. From the images, the timeframe for complete crystallization of the PLA was the longest at this temperature, taking 15 minutes before all spherulites had impinged on one another. This time was reduced by half in the case of the plasticizer as the PEG boosts the spherulitic growth rate of PLA by increasing chain mobility [47]. No visible alternation in the spherulitic size of the PLA/PEG blend occurred, which relates to the nucleation density remaining the same. However, in the case of the nucleating agent samples with and without the inclusion of PEG, the crystallization was too

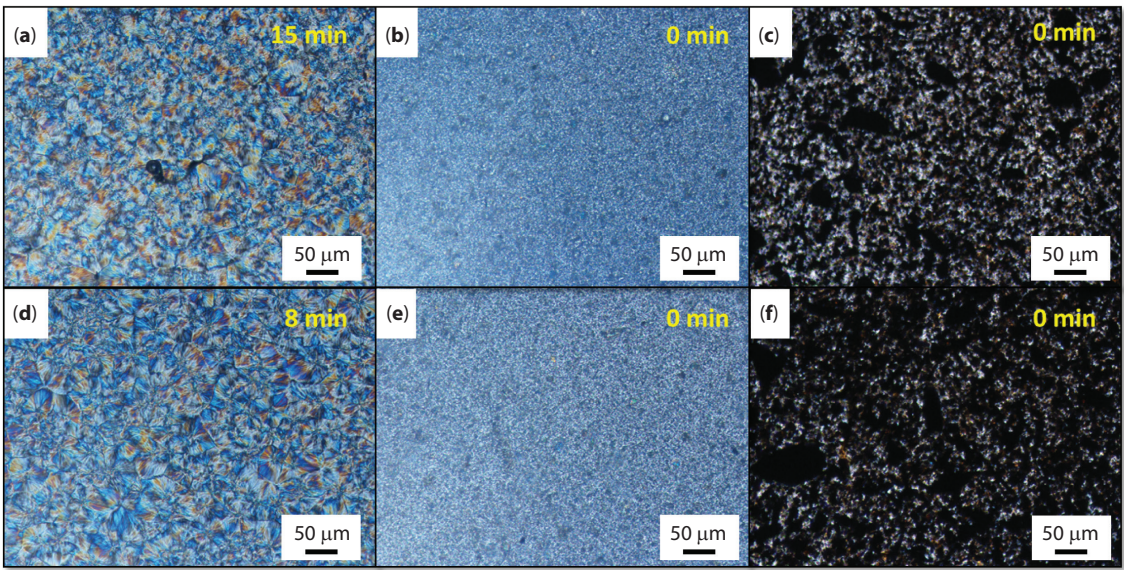

Figure 8 Polarized optical microscope images of the crystallized samples of (**a**) PLA, (**b**) PLA/Talc, (**c**) PLA/BC, (**d**) PLA/PEG, (**e**) PLA/PEG/Talc, (f) PLA/PEG/BC and the times before complete crystallization at 120 °C.

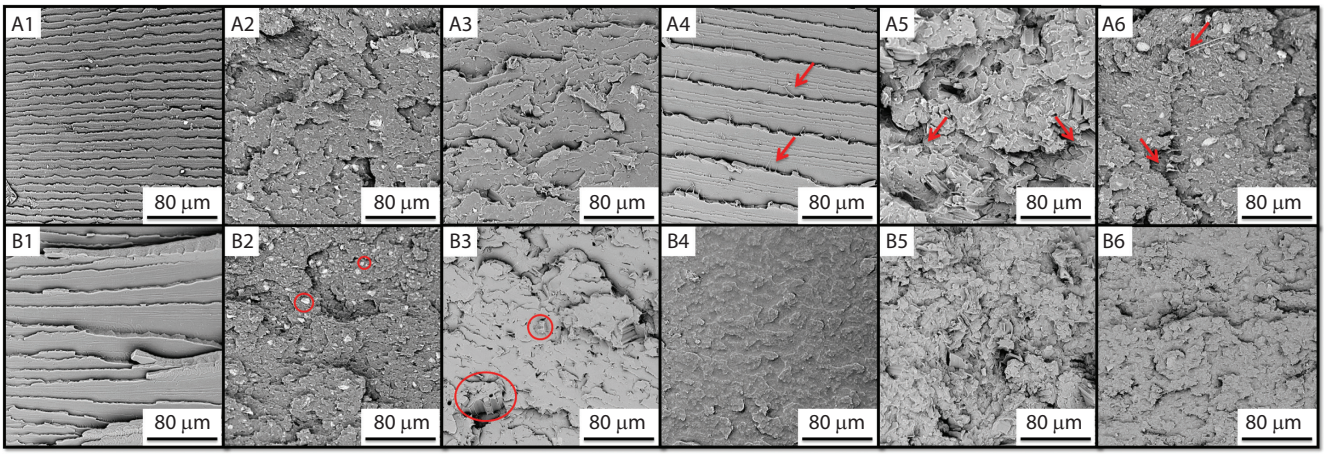

Figure 9 SEM topography of impact fractured surfaces of (A) 48 °C molded samples (1) PLA, (2) PLA/Talc, (3) PLA/Biocarbon, (4) PLA/PEG, (5) PLA/PEG/Biocarbon, and (6) PLA/PEG/Talc, along with the (B) 90 °C molded samples.

fast to observe at this isothermal crystallization temperature. These samples showed a large reduction in spherulitic size as the nucleation density was drastically increased. The talc and biocarbon functioned as nucleation sites for the PLA crystallization and with a greater number of crystal nuclei, space confinement during crystal growth culminated in smaller spherulites [48].

The impact fracture surfaces of the PLA-based samples are illustrated in Figure 9. Brittle fracture surfaces are apparent for the neat PLA samples and low mold temperature PLA/PEG sample. These samples show fracture steps in the direction of crack propagation. Only the samples containing the plasticizer at low mold temperature show some ductile characteristics, with the arrows pointing to several polymeric strands that have been elongated, which may have contributed to the slight increase in impact strength observed for those ternary blends. These microfibrils were not present in the high mold temperature PEG-containing samples as the crystallinity of these samples gave the material a fragile quality, as seen with the smoother surface topographies than the low molded PEG samples. The surface images of the talc or biocarbon composites have a rougher nature to them with several nucleating agents circled to show the difference in size and shape. These rigid nucleating agents impeded the crack tip, absorbing a small amount of the impact energy during crack propagation through the matrix, contributing to the coarser surface profiles of the composites.

4 CONCLUSIONS

This research probed how the inclusion of plasticizer and nucleating agents affected the PLA crystallinity in an injection molding setting, with the general trends displayed in Table 3. Findings showed that the plasticizer poly(ethylene glycol) was beneficial in imparting more mobility for the PLA chains to form crystals. The biocarbon impeded the crystal growth on its own but strengthened the crystallinity when complemented with the plasticizer. The talc nucleating agent, generally used, performed well at high mold temperatures, especially without the use of PEG. The optimum composite formulations provided PLA with the maximum crystallinity, having no cold crystallization. These injection molded samples did, however, require the higher mold temperature of 90 °C to attain these properties and had some loss in mechanical strength. The fully crystalline PLA samples provided thermal stability in terms of HDT above 100 °C and CLTE reduction by 30–35%. The undervalued biobased carbon showed the ability to act as a less dense alternative nucleating agent compared to talc when injection molded at a high mold temperature with plasticizer present.

ACKNOWLEDGMENTS

This research is financially supported by the Ontario Ministry of Agriculture, Food, and Rural Affairs (OMAFRA) – New Directions Research Program (Project # 049528); the Natural Sciences and Engineering Research Council (NSERC), Canada Discovery grant (Project # 400320 and # 401111); and the Ontario Research Fund, Research Excellence Program – Round-7 (ORF-RE07) from the Ontario Ministry of Research and Innovation, currently known as the Ontario Ministry of Research, Innovation and Science (MRIS) (Project # 052644 and # 052665).

Table 3 Main trends observed for the PLA samples.

Additives		**Mold temperature**	
		Low (48 °C)	**High (90 °C)**
Plasticizer	PEG	• T_g, HDT, and modulus reduced • %χ and CLTE increased	• HDT no change • T_g and modulus reduced • %χ and CLTE increased
Nucleating Agents	Talc	• T_g and HDT no change • CLTE reduced • %χ and modulus increased	• T_g no change • CLTE reduced • %χ, HDT, and modulus increased
	Biocarbon	• T_g, %χ, and HDT no change • CLTE and modulus increased	• T_g, %χ, and HDT no change • CLTE and modulus increased
Plasticizer + Nucleating Agent	PEG + Talc	• T_g, HDT, and modulus reduced • %χ and CLTE increased	• T_g, CLTE, and modulus reduced • %χ and HDT increased
	PEG + Biocarbon		

REFERENCES

1. L.-I. Palade, H.J. Lehermeier, and J.R. Dorgan, Melt rheology of high L-Content Poly(lactic acid). *Macromolecules* **34**(5), 1384–1390 (2001).
2. O. Martin and L. Avérous, Poly(lactic acid): Plasticization and properties of biodegradable multiphase systems. *Polymer (Guildf.)* **42**(14), 6209–6219 (2001).
3. A. Galeski, Strength and toughness of crystalline polymer systems. *Prog. Polym. Sci.* **28**(12), 1643–1699 (2003).
4. T. Tabi, Crystalline structure of annealed polylactic acid and its relation to processing. *eXPRESS Polym. Lett.* **4**(10), 659–668 (2010).
5. H. Tsuji and Y. Ikada, Crystallization from the melt of poly(lactide)s with different optical purities and their blends. *Macromol. Chem. Phys.* **197**(10), 3483–3499 (1996).
6. A.M. Harris and E.C. Lee, Improving mechanical performance of injection molded PLA by controlling crystallinity. *J. Appl. Polym. Sci.* **107**(4), 2246–2255 (2008).
7. T.J. Bessell, D. Hull, and J.B. Shortall, The effect of polymerization conditions and crystallinity on the mechanical properties and fracture of spherulitic nylon 6. *J. Mater. Sci.* **10**(7), 1127–1136 (1975).
8. R.J. Crawford, *Plastics Engineering*, 3rd ed. Elsevier Butterworth-Heinemann, Oxford, UK (1998).
9. D. Yao and B. Kim, Development of rapid heating and cooling systems for injection molding applications. *Polym. Eng. Sci.* **42**(12), 2471–2481 (2002).
10. T.L. Smith, D. Masilamani, L.K. Bui, R. Brambilla, Y.P. Khanna, and K.A. Garbriel, Acetals as nucleating agents for polypropylene. *J. Appl. Polym. Sci.* **52**(5), 591–596 (1994).
11. N. Kawamoto, A. Sakai, T. Horikoshi, T. Urushihara, and E. Tobita, Nucleating agent for poly(L-lactic acid)—An optimization of chemical structure of hydrazide compound for advanced nucleation ability. *J. Appl. Polym. Sci.* **103**(1), 198–203 (2007).
12. N. Petchwattana, S. Covavisaruch, and S. Petthai, Influence of talc particle size and content on crystallization behavior, mechanical properties and morphology of poly(lactic acid). *Polym. Bull.* **71**(8), 1947–1959 (2014).
13. M. Rahman and C. Brazel, The plasticizer market: An assessment of traditional plasticizers and research trends to meet new challenges. *Prog. Polym. Sci.* **29**(12), 1223–1248 (2004).
14. N. Ljungberg and B. Wesslén, The effects of plasticizers on the dynamic mechanical and thermal properties of poly(lactic acid). *J. Appl. Polym. Sci.* **86**(5), 1227–1234 (2002).
15. S. Saeidlou, M.A. Huneault, H. Li, and C.B. Park, Poly(lactic acid) crystallization. *Prog. Polym. Sci.* **37**(12), 1657–1677 (2012).
16. C. Liu and M. Muthukumar, Langevin dynamics simulations of early-stage polymer nucleation and crystallization. *J. Chem. Phys.* **109**(6), 2536–2542 (1998).
17. S. Ghosh, J.C. Viana, R.L. Reis, and J.F. Mano, Effect of processing conditions on morphology and mechanical properties of injection-molded poly(l-lactic acid). *Polym. Eng. Sci.* **47**(7), 1141–1147 (2007).
18. H. Li and M. A. Huneault, Effect of nucleation and plasticization on the crystallization of poly(lactic acid). *Polymer (Guildf.)* **48**(23), 6855–6866 (2007).
19. V. Nagarajan, A.K. Mohanty, and M. Misra, Biocomposites with size-fractionated biocarbon: Influence of the microstructure on macroscopic properties. *ACS Omega* **1**(4), 636–647 (2016).
20. Standard test method for tensile properties of plastics, ASTM D638-14 (2014).
21. Standard test methods for flexural properties of unreinforced and reinforced plastics and electrical insulating materials, ASTM D790-15 (2016).
22. Standard test methods for determining the izod pendulum impact resistance of plastics, ASTM D256-10 (2015).
23. Standard test method for deflection temperature of plastics under flexural load in the edgewise position, ASTM D648-16 (2016).
24. Standard test method for linear thermal expansion of solid materials by thermomechanical analysis, ASTM E831-14 (2014).
25. E.W. Fischer, H.J. Sterzel, and G. Wegner, Investigation of the structure of solution grown crystals of lactide copolymers by means of chemical reactions. *Kolloid-Zeitschrift und Zeitschrift für Polym.* **251**(11), 980–990 (1973).
26. B.-S. Park, J.C. Song, D.H. Park, and K.-B. Yoon, PLA/chain-extended PEG blends with improved ductility. *J. Appl. Polym. Sci.* **123**(4), 2360–2367 (2012).
27. Z. Kulinski and E. Piorkowska, Crystallization, structure and properties of plasticized poly(l-lactide). *Polymer (Guildf.)* **46**(23), 10290–10300 (2005).
28. D. Battegazzore, Crystallization kinetics of poly(lactic acid)-talc composites. *Express Polym. Lett.* **5**(10), 849–858 (2011).
29. M.T. Takemori, Towards an understanding of the heat distortion temperature of thermoplastics. *Polym. Eng. Sci.* **19**(15), 1104–1109 (1979).
30. S. Cheng, K. Lau, T. Liu, Y. Zhao, P.-M. Lam, and Y. Yin, Mechanical and thermal properties of chicken feather fiber/PLA green composites. *Compos. Part B Eng.* **40**(7), 650–654 (2009).
31. P.J. Yoon, T.D. Fornes, and D.R. Paul, Thermal expansion behavior of nylon 6 nanocomposites. *Polymer (Guildf.)* **43**(25), 6727–6741 (2002).
32. J.F. Balart, D. García-Sanoguera, R. Balart, T. Boronat, and L. Sánchez-Nacher, Manufacturing and properties of biobased thermoplastic composites from poly(lactid acid) and hazelnut shell wastes. *Polym. Compos.* DOI: 10.1002/pc.24007 (2016).
33. Y.P. Mamunya, V.V. Davydenko, P. Pissis, and E.V. Lebedev, Electrical and thermal conductivity of polymers filled with metal powders. *Eur. Polym. J.* **38**(9), 1887–1897 (2002).
34. B. Weidenfeller, M. Höfer, and F.R. Schilling, Thermal conductivity, thermal diffusivity, and specific heat capacity of particle filled polypropylene. *Compos. Part A Appl. Sci. Manuf.* **35**(4), 423–429 (2004).
35. S. Radhakrishnan, P. Sonawane, and N. Pawaskar, Effect of thermal conductivity and heat transfer on crystallization, structure, and morphology of polypropylene

containing different fillers. *J. Appl. Polym. Sci.* **93**(2), 615–623 (2004).
36. T. Tábi, A. Suplicz, T. Czigány, and J.G. Kovács, Thermal and mechanical analysis of injection moulded poly(lactic acid) filled with poly(ethylene glycol) and talc. *J. Therm. Anal. Calorim.* **118**(3), 1419–1430 (2014).
37. A.C. Fowlks and R. Narayan, The effect of maleated polylactic acid (PLA) as an interfacial modifier in PLA-talc composites. *J. Appl. Polym. Sci.* **118**(5), 2810–2820 (2010).
38. M. Pluta, Morphology and properties of polylactide modified by thermal treatment, filling with layered silicates and plasticization. *Polymer (Guildf.)* **45**(24), 8239–8251 (2004).
39. S. Ahmed and F.R. Jones, A review of particulate reinforcement theories for polymer composites. *J. Mater. Sci.* **25**(12), 4933–4942 (1990).
40. B.L. Shah and V.V. Shertukde, Effect of plasticizers on mechanical, electrical, permanence, and thermal properties of poly(vinyl chloride). *J. Appl. Polym. Sci.* **90**(12), 3278–3284 (2003).
41. J.R. Sarasua, A.L. Arraiza, P. Balerdi, and I. Maiza, Crystallinity and mechanical properties of optically pure polylactides and their blends. *Polym. Eng. Sci.* **45**(5), 745–753 (2005).
42. M.-Y. Jo, Y.J. Ryu, J.H. Ko, and J.-S. Yoon, Hydrolysis and thermal degradation of poly(L-lactide) in the presence of talc and modified talc. *J. Appl. Polym. Sci.* **129**(3), 1019–1025 (2013).
43. S. Wong, R.A. Shanks, and A. Hodzic, Mechanical behavior and fracture toughness of poly(L-lactic acid)-natural fiber composites modified with hyperbranched polymers. *Macromol. Mater. Eng.* **289**(5), 447–456 (2004).
44. B. Wetzel, F. Haupert, K. Friedrich, M.Q. Zhang, and M.Z. Rong, Impact and wear resistance of polymer nanocomposites at low filler content. *Polym. Eng. Sci.* **42**(9), 1919–1927 (2002).
45. Y.W. Leong, M.B. Abu Bakar, Z.A.M. Ishak, A. Ariffin, and B. Pukanszky, Comparison of the mechanical properties and interfacial interactions between talc, kaolin, and calcium carbonate filled polypropylene composites. *J. Appl. Polym. Sci.* **91**(5), 3315–3326 (2004).
46. A. El-Hadi, R. Schnabel, E. Straube, G. Müller, and S. Henning, Correlation between degree of crystallinity, morphology, glass temperature, mechanical properties and biodegradation of poly (3-hydroxyalkanoate) PHAs and their blends. *Polym. Test.* **21**(6), 665–674 (2002).
47. H. Xiao, W. Lu, and J.-T. Yeh, Effect of plasticizer on the crystallization behavior of poly(lactic acid). *J. Appl. Polym. Sci.* **113**(1), 112–121 (2009).
48. H.W. Xiao, P. Li, X. Ren, T. Jiang, and J.-T. Yeh, Isothermal crystallization kinetics and crystal structure of poly(lactic acid): Effect of triphenyl phosphate and talc. *J. Appl. Polym. Sci.* **118**(6), 3558–3569 (2010).